Arch. Metall. Mater. **66** (2021), 2, 503-510

DOI: 10.24425/amm.2021.135885

S. GARUS[1*], W. SOCHACKI[1]

THE EFFECT OF LAYER THICKNESS ON THE REFLECTANCE OF A QUASI ONE-DIMENSIONAL COMPOSITE BUILT WITH $Zr_{55}Cu_{30}Ni_5Al_{10}$ AMORPHOUS ALLOY AND EPOXY RESIN

The study examined the impact of the angle of incidence of mechanical waves on various types of quasi one-dimensional superlattice. Binary periodic structure, quasi-periodic distribution of Thue-Morse layers and Severin's aperiodic multilayer were used. Using the concatenation and recursive rules, the distribution of layers was determined for individual structure types for generation numbers equal to 3, 4 and 5. The structures were selected so that the thickness of the composite was the same for each type of distribution for a given generation number value. Transfer Matrix Method algorithm was used to determine reflectance. The band structure of reflectance has been demonstrated for incidence angles up to 90 degrees at mechanical wave frequencies up to 50 kHz. The existence of wide bands of high reflectance above the acoustic frequencies was demonstrated for the analyzed structures. Increasing the layer thickness caused an inhomogeneous shifts of transmission peaks towards lower frequencies.

Keywords: amorphous alloy, aperiodic multilayer, mechanical waves, phononic crystal, bandgap

1. Introduction

Acoustic mirrors have been called phononic constructions with high reflectance. In addition to materials with natural properties that reflect acoustic waves, structures (PnC phononic crystals) are increasingly being created in which waves with specific frequencies will not propagate. The phenomenon of the lack of wave propagation at given frequencies is called the occurrence of a phononic bandgap (PhBG). The band gap width depends on the crystal structure and the type of used materials. In addition, the position and bandwidth of the bandgap depend on the direction of propagation, because the path difference depends on the angle of incidence [1]. In some PnC structures, bandgaps occur for any propagation direction and are called full bandgaps. Over the past several years, many interesting studies have been conducted on the bandgap characteristic of phononic crystals [2-7]. In the review [8] Pennec et al. presented interesting applications of two-dimensional phononic crystals. The work contains very extensive literature on PnC. PnC potential applications include acoustic diodes (Li et al. [9]), waveguides (Khelif et al. [10]), noise suppressors (Richards and Pines [11]), ultrasonic and polarizing filters (Kafesaki et al. [12]) or acoustic barriers (Sanchez-Perez et al. [13]). Many authors conduct research that focuses on PnC design to achieve an "appropriate" band gap. Some authors have attempted to design phononic crystals in such a way as to suppress waves of a certain frequency (Alagoz et al. [14]). Still others tried to get a perfect reflection of the sound wave by obtaining an exceptionally wide bandgap (Bilal and Hussein [15]).

Many authors have studied the reflectance of phononic crystals. An analysis of the reflectance of sonic crystals consisting of square arrays of rigid cylinders in air is presented in [16]. The article [17] presents structures characterized by a wide reflection range for ultrasonic mechanical waves. A lot of research in this area concerns acoustic screens built on the basis of phononic crystals [13,18]. Interesting studies on acoustic barriers were conducted by the authors of the paper [19]. In this article, the sound crystal barrier, enriched with rubber crumbs inside micro-perforated cylindrical coatings, was characterized using standard measuring techniques in accordance with EN 1793-5 and EN 1793-6. Based on EN 1793-6 Morandi et al. [20] characterized the acoustic barrier for which it was shown that the values of sound insulation index and reflection coefficient strongly depend on the measurement configuration.

In previous studies, the authors mostly analyzed the reflection and scattering of a mechanical wave incident on a phononic

[1] CZESTOCHOWA UNIVERSITY OF TECHNOLOGY, DEPARTMENT OF MECHANICS AND FUNDAMENTALS OF MACHINERY DESIGN, FACULTY OF MECHANICAL ENGINEERING AND COMPUTER SCIENCE, 73 DĄBROWSKIEGO STR., 42-201 CZĘSTOCHOWA, POLAND

* Corresponding author: gari.sg@gmail.com

crystal without taking into account the variable angle of incidence of the wave. Few works in this field are, for example, works [21 and 22]. In [21], the authors examined sound transfer characteristics in a single-layer acoustic mesh built using cells of the metamaterial unit. They confirmed that the interference of the wave depends on its frequency, which is highly dependent on the periodicity of the grid and the angle of incidence of the wave. In another work [22], angular control of incident sound waves was examined for total transmission and inverted reflection using phonon crystals. Based on changes in the position of the Dirac point, which regularly changes with the ratio of length to width of the rubber rods used in PnC, the transmission angle can be adjusted.

2. Materials and methods

In this work, the reflection coefficient for three types of quasi one-dimensional structures with the same number of layers was examined. They were respectively: periodic – binary, quasi-periodic – Thue-Morse and aperiodic – Severin. The influence of the mechanical wave angle of incidence on the existence of reflection bands in the range of sounds and ultrasounds was analyzed in detail. The Transfer Matrix Method (TMM) algorithm was used to analyze the wave reflectance in the examined structures.

2.1. Transfer Matrix Method

The TMM algorithm is widely used in physical modeling due to its speed. The TMM algorithm used allows mathematical description of the wave transmission and reflection coefficient through the multilayer medium. Each layer of such a medium (Fig. 1) has an infinite range in lateral directions. At the layer boundaries, wave propagation continuity conditions are taken into account. The mechanical wave falling on the structure is defined as $p_{in}^{(+)}$, the reflected wave is $p_{in}^{(-)}$, the wave passing through the structure is $p_{out}^{(+)}$. The d_i is the thickness of the x_i layer.

The method used is very convenient because the mathematical description of the wave propagation in the layer is done by matrix multiplication, and the physical quantities of different media can be coupled through interface matrices.

Using TMM can be determine the reflection and transmission coefficients of multilayer structures, which was proposed in their work by Dazel et al. [23]. For the analysis of three multilayer structures with a defect in the form of a piezoelectric layer, the TMM algorithm was used by Garus et al. [24]. Propagation of elastic waves in disordered multilayer structures made of two different materials was studied by Sigalas and Soukoulis [25] using TMM. In [26], the authors investigated (using TMM) the problem of acoustic wave propagation in a one-dimensional water channel containing many air blocks. Garus and Sochacki [27] based their research on TMM and FDTD algorithms, determining power spectrum and phononic properties of Severin's quasi one-dimensional aperiodic structure. The TMM method was also used by Pop and Cretu [28] to analyze the longitudinal propagation of 1D elastic wave by multilayer media to obtain equivalent split quaternion formalism. The paper [29] presents transmission in quasi-one-dimensional structures taking into account different angles of incidence of the wave.

Wave propagation in a multilayer medium is described by a differential equation

$$\frac{1}{v_i^2}\frac{\partial^2 p}{\partial t^2} - \nabla^2 p = 0 \tag{1}$$

where t is a time, p is the an acoustic wave pressure, and v_i is a phase velocity in layer i. For a quasi one-dimensional structure, the solution to the above equation takes the form

$$p_i = \left(A_i e^{jk_i x} + B_i e^{-jk_i x}\right) e^{-j\omega t} = C_i(x) e^{-j\omega t} \tag{2}$$

Coefficients A_i and B_i determine respectively the amplitude of the wave propagating with the incident wave direction and the amplitude of the wave propagating in the opposite direction. in a given layer i (where $j = \sqrt{-1}$). The wave vector k_i depends on the phase velocity v_i of the wave in the material of the layer i and the frequency f of the propagating wave

$$k_i = \frac{2\pi f}{v_i} \tag{3}$$

Reflection coefficient R can be determined for lossless materials from the transmission coefficient T

$$R = 1 - T \tag{4}$$

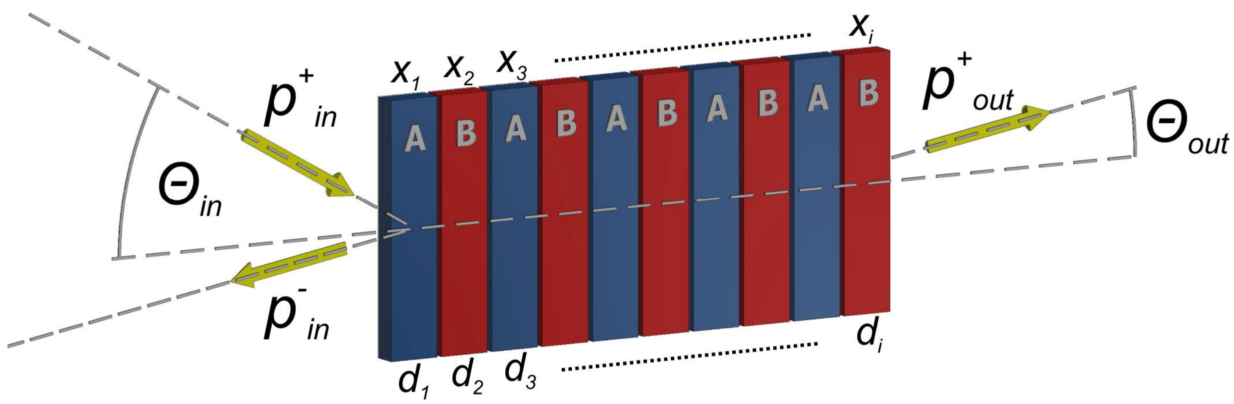

Fig. 1. Multilayer structure in TMM algorithm

$$T = \frac{Z_{in}\cos\Theta_{out}}{Z_{out}\cos\Theta_{in}}\left|\frac{1}{\Gamma_{1,1}}\right|^2 \tag{5}$$

where Z_{in} is the acoustic impedance of the medium from which the wave penetrates the structure at an angle Θ_{in} to normal to the surface of the multilayer, while Z_{out} is the acoustic impedance of the medium in which the wave propagates after leaving the structure at the angle of Θ_{out}.

The transmission T is determined from the characteristic matrix Γ appearing in the matrix equation describing the propagation of a mechanical wave in a multilayer structure, where p_{in}^+ represents incident wave, p_{in}^- reflected and p_{out}^+ transmitted

$$\begin{bmatrix} p_{in}^+ \\ p_{in}^- \end{bmatrix} = \Gamma \begin{bmatrix} p_{out}^+ \\ 0 \end{bmatrix} \tag{6}$$

The characteristic matrix Γ is defined as

$$\Gamma = D_{in}^{-1}\left[\prod_{i=1}^{n} D_i P_i D_i^{-1}\right] D_{out} \tag{7}$$

The P_i matrix describing propagation in a single layer i for a given thickness d_i and is described as

$$P_i = \begin{bmatrix} e^{jk_i d_i \cos\Theta_i} & 0 \\ 0 & e^{-jk_i d_i \cos\Theta_i} \end{bmatrix} \tag{8}$$

The transmission matrix D_i is defined by

$$D_i = \begin{bmatrix} 1 & 1 \\ \dfrac{\cos\Theta_i}{Z_i} & -\dfrac{\cos\Theta_i}{Z_i} \end{bmatrix} \tag{9}$$

and depends on the acoustic impedance Z_i and the angle of wave propagation Θ_i in a given layer i.

2.2. Materials

The work analyzes structures made of lossless materials. Amorphous alloys are intensively studied due to their special properties (e.g. magnetic [30-32]), while their structure is important, due to which the mechanical wave propagates isotropically. Material A was an amorphous alloy $Zr_{55}Cu_{30}Ni_5Al_{10}$ with mechanical wave phase velocity equal to 1633 [m/s] and mass density equal to 6829 [kg·m^{-3}] [33]. Epoxy resins were adopted as material B (density is 1180 [kg·m^{-3}] and phase velocity 2535 [m/s]) [34]. In the second considered case, epoxy resin was assigned to material A and amorphous alloy to material B. The external environment was water with a mass density of 1000 [kg·m^{-3}] and phase velocity 1480 [m/s] [34]. The materials were selected in such a way that they significantly differ in their acoustic impedance values.

2.3. Analyzed structures

The study analyzes mechanical wave propagation in binary, aperiodic (Severin [35]) and quasi-periodic (Thue-Morse [36]) structures. The structures have been selected so that for a given generation number $L = \{3,4,5\}$ they have the same number of layers, and the entire multilayer the same thickness. Thanks to this, only the influence of layer distribution is analyzed. The arrangement of layers in the structure of the periodic binary superlattice is determined by the concatenation rule

$$X_L^B = (AB)^{2^{L-1}} \tag{10}$$

where for the next generation number L the initiation string $X_1^B = AB$ is repeated 2^{L-1} times. For generation numbers $L = \{3,4,5\}$, the distribution of layers is as follows

$$X_3^B = ABABABAB,\ X_4^B = ABABABABABABABAB$$

and

$$X_5^B = ABABABABABABABABABABABABABABABAB.$$

The other two layer distributions were created according to the recursive rule. For the Thue-Morse structure, the initial chain is $X_0^{T-M} = A$ while the next generations X_L^{T-M} are created according to the relationship

$$\begin{cases} A \to AB \\ B \to BA \end{cases} \tag{11}$$

which gives accordingly

$$X_3^{T-M} = ABBABAAB,\ X_4^{T-M} = ABBABAABBAABABBA$$

and

$$X_5^{T-M} = ABBABAABBAABABBABAABABBAABBABAAB.$$

Whereas in Severin's structure X_L^S the initiation chain is $X_0^S = B$ and the recursive rule is defined as

$$\begin{cases} A \to BB \\ B \to AB \end{cases} \tag{12}$$

Generated Severin's structures takes the form

$$X_3^S = ABABBBAB,\ X_4^S = BBABBBABABABBBAB$$

and

$$X_5^S = ABABBBABABABBBABBBABBBABABABBBAB.$$

2.4. The surface impedance of the structure

The surface impedance of the structure [37], can be calculated by equation

$$Z_S = Z_0\frac{1+R}{1-R} = Z_0 M \tag{13}$$

Where Z_0 is acoustic impedance of the external environment and R is a reflectance. In the analyzed structures, the reflectance in the band gaps frequency range is close to 1, which means that the value of the fraction M increases significantly and the acoustic impedance value increases with it. Due to the large variation in the value of the M coefficient, the value of its decimal logarithm is given.

3. Results

The use of Transfer Matrix Method algorithm allowed to determine the reflectance of the analyzed structures where material A was an amorphous alloy $Zr_{55}Cu_{30}Ni_5Al_{10}$ and material B was epoxy resin. Wave propagation in the frequency range up to 50 kHz and the angle of incidence up to 90 degrees was studied. The results are collected in Figure 2. The maximum reflectance is marked in white on the charts, while the full transmission through the structure is marked by black.

As shown in Figure 2, there are large areas of high reflection for higher frequencies. However, for lower frequencies, the reflectance has a band structure. As the number of layers increases, the number of low reflectance bands for low frequencies increases, while the half bandwidth decreases. Attention should be paid to the occurrence of narrow bands of low reflectance in the higher frequency range for structures in which there is no translational order of layers. In the binary structure, as the number of layers increased, the area of full reflectance decreased. For the 4th and 5th generation numbers in the Thue-Morse and Severin superlattices there were high reflectance bands in the acoustic frequency range.

In order to examine the influence of material selection for the structure on the reflectance of multilayers, tests were carried out where material A was epoxy resin while material B was amorphous alloy. The results are collected in Figure 3. When changing materials, the reflectance structure for binary and Thue-Morse (for L equal to 3 and 5 – Figs 3d and 3f) superlattice has not changed. The reflectance characteristics for the other structures showed changes.

Then, an analysis of the effect of layer thickness on reflectance was carried out. The X_5^{T-M} structure was selected for

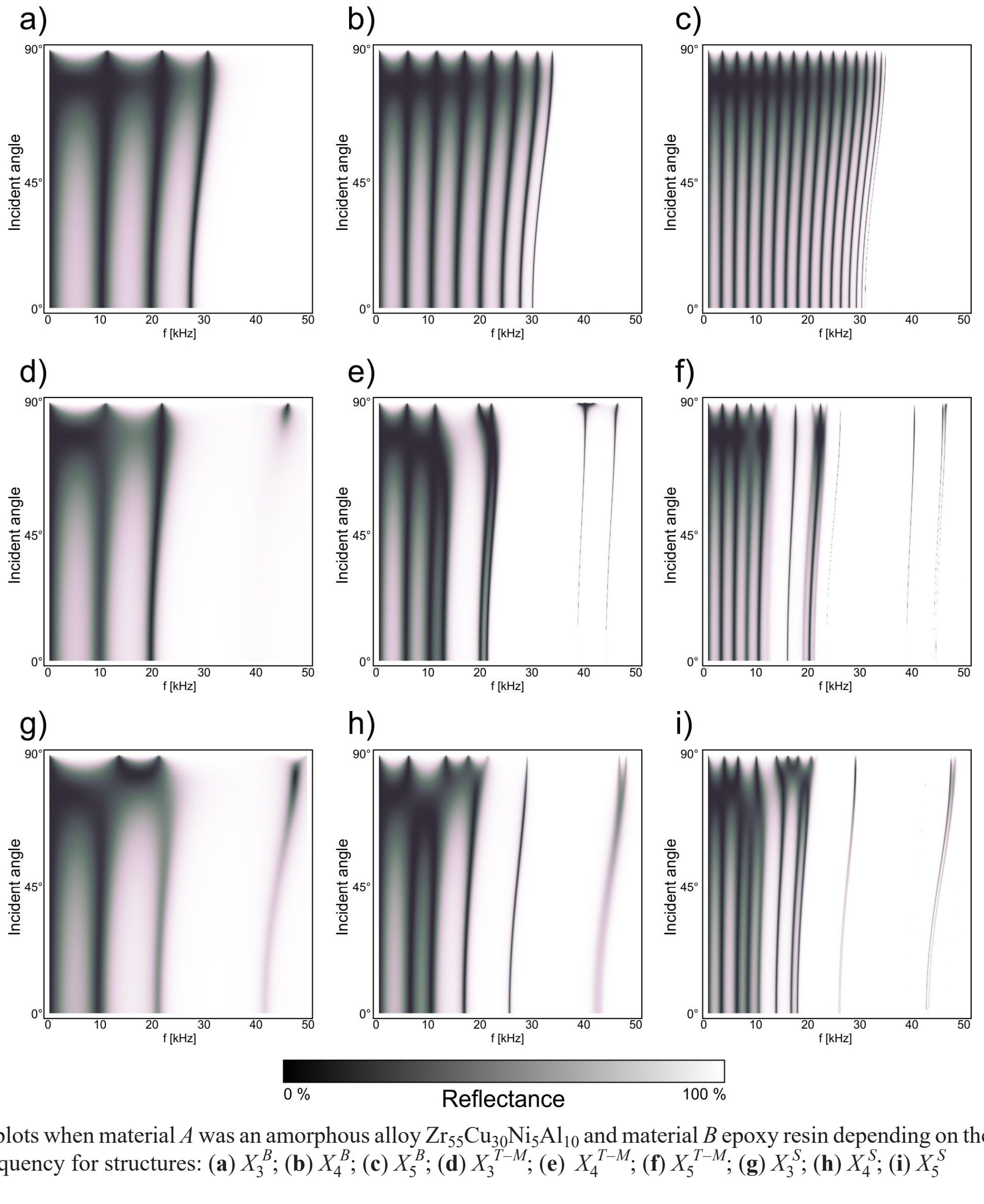

Fig. 2. Reflectance plots when material A was an amorphous alloy $Zr_{55}Cu_{30}Ni_5Al_{10}$ and material B epoxy resin depending on the angle of incidence of the wave and frequency for structures: (**a**) X_3^B; (**b**) X_4^B; (**c**) X_5^B; (**d**) X_3^{T-M}; (**e**) X_4^{T-M}; (**f**) X_5^{T-M}; (**g**) X_3^S; (**h**) X_4^S; (**i**) X_5^S

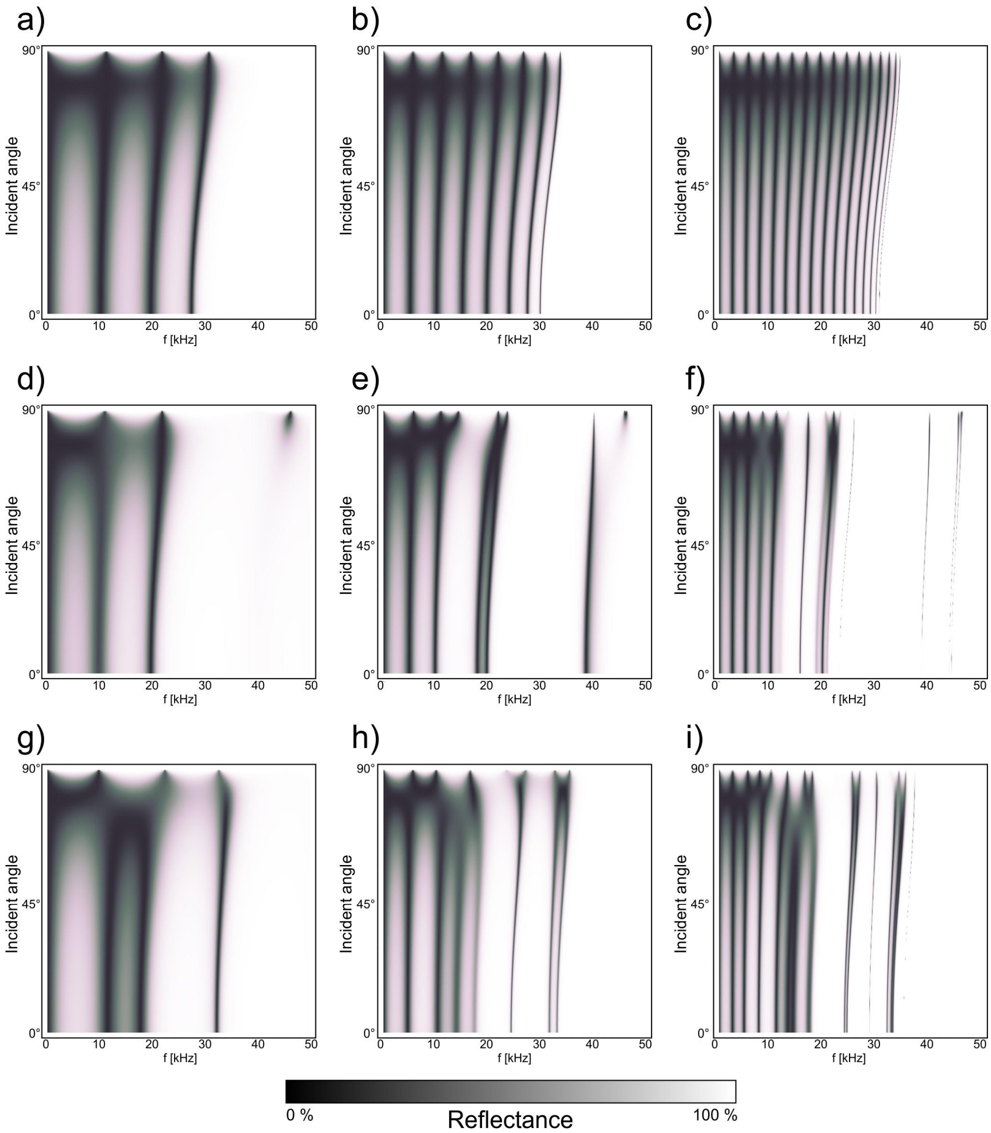

Fig. 3. Reflectance plots when material *A* was epoxy resin and material *B* an amorphous alloy $Zr_{55}Cu_{30}Ni_5Al_{10}$ depending on the angle of incidence of the wave and frequency for structures: (**a**) X_3^B; (**b**) X_4^B; (**c**) X_5^B; (**d**) X_3^{T-M}; (**e**) X_4^{T-M}; (**f**) X_5^{T-M}; (**g**) X_3^S; (**h**) X_4^S; (**i**) X_5^S

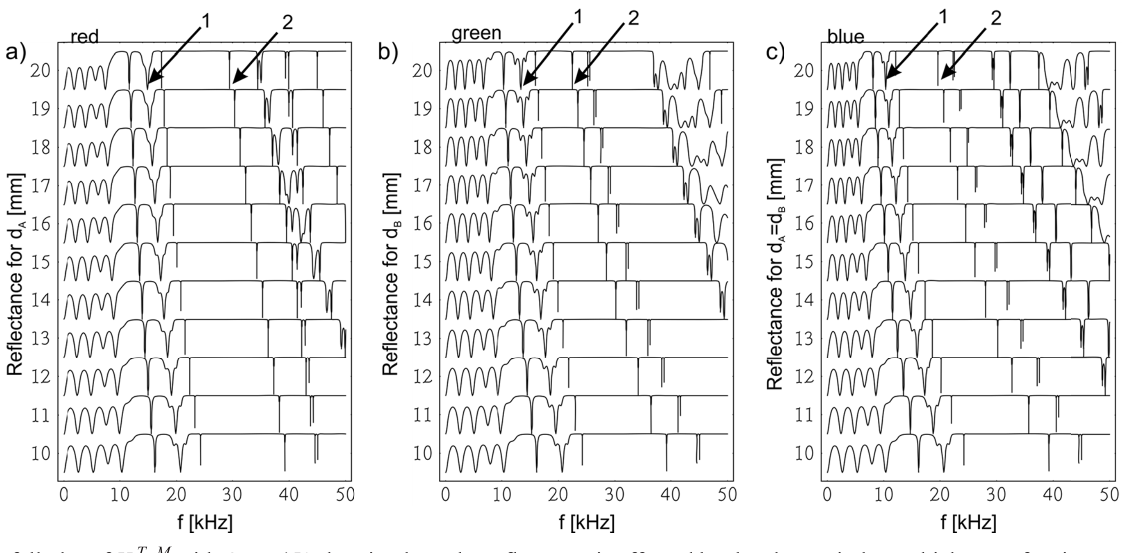

Fig. 4. Waterfall plot of X_5^{T-M} with $\Theta_{in} = 45°$ showing how the reflectance is affected by the change in layer thickness of a given type: (**a**) layer A thickness change in the range from 10 mm to 20 mm in 1 mm increments, layer B with a constant thickness of 10 mm (**b**) layer B thickness change in the range from 10 mm to 20 mm in 1 mm increments, layer A with a constant thickness of 10 mm; (**c**) layer A and layer B thickness change in the range from 10 mm to 20 mm in 1 mm increments. The numbers 1 and 2 indicate the transmission peaks whose shifts have been analyzed

analysis because the reflectance structure was independent of the assigned materials for the layers, the number of type A layers was the same as type B layers and showed a large number of narrow high transmission peaks. The analysis was performed for the angle $\Theta_{in} = 45°$. Figure 4a shows how the change in the thickness of layer A (epoxy resin) affected the reflectance structure. As the A layers thickness value increased, the transmission peaks shifted towards lower frequencies. Similar transmission peak shifts occurred when only increasing the thickness of layer B (Fig. 4b) and while increasing the thickness of both layers (Fig. 4c). Figure 5 shows how the transmission peaks marked in Figure 4 shifts as the layer thickness increases, the colors listed in Figure 4 correspond to the colors of the line in Figure 5.

Figure 6 shows an exemplary reflectance spectrum of the X_3^{T-M} structure for a mechanical wave incident at the $\Theta_{in} = 45°$ angle. It should be noted that for the band gap above 30 kHz, there is a sharp increase in the coefficient M in Equation 13, and thus also a sharp increase in the acoustic impedance of the surface of the structure under study. Figure 7 shows the values of the decimal logarithm of the M parameter, showing the proportional increase in the value of the surface acoustic impedance of the analyzed structures in relation to the acoustic impedance of the medium. For each type of structure, an increase in the acoustic impedance of the surface was observed with the increase in the number of layers.

4. Discussion

The work analyzed mechanical wave reflectance in quasi one-dimensional phononic structures. binary structure showing periodic invariance, quasi-periodic Thue-Morse and Severin's aperiodic structures. The band nature of reflectance has been demonstrated for all multilayers and the impact of the angle of incidence on transmission peak shifts. Increasing the number of layers caused an increase in the number of transmission peaks and a reduction in their half width. The aperiodic structure of the multilayers resulted in the formation of a forbidden gap at lower frequency values, although narrow peaks of high transmission in the higher frequency range were also formed then. The change of materials in the structure of the multilayer did not affect the reflectance in the periodic table, while it changed the nature of the reflectance for Severin superlattice. In the case of the distribution of Thue-Morse layers, the change of materials affected

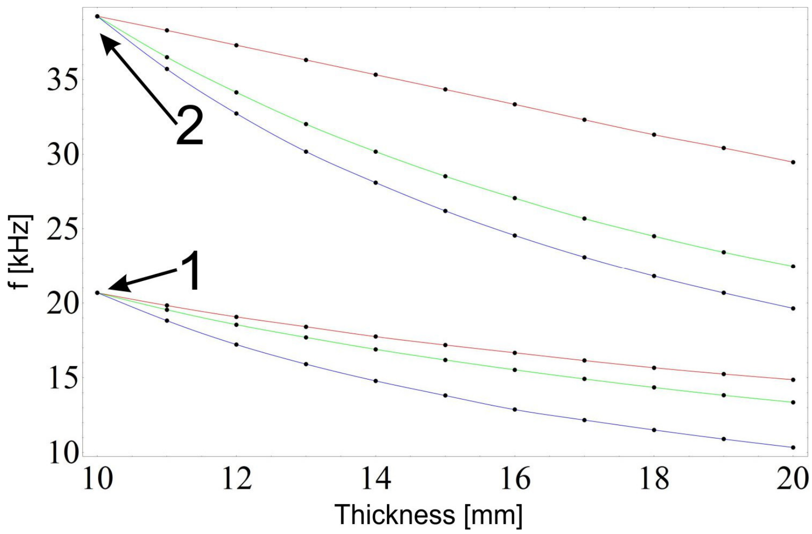

Fig. 5. Transmission peak shifts with increasing layer thickness in the X_5^{T-M} structure for the mechanical wave incident at $\Theta_{in} = 45°$angle

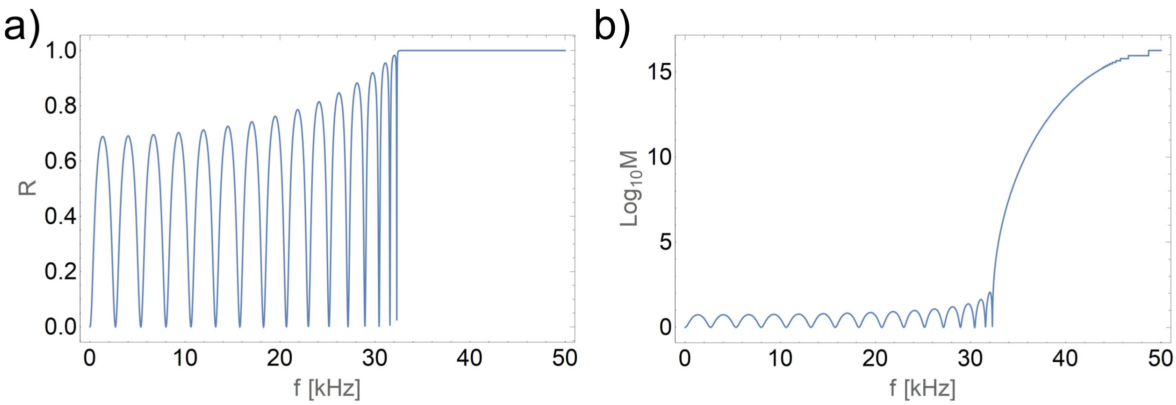

Fig. 6. Reflectance (a) for the X_3^{T-M} structure and the $\Theta_{in} = 45°$ angle of incidence and the corresponding value of the decimal logarithm of the coefficient M (b)

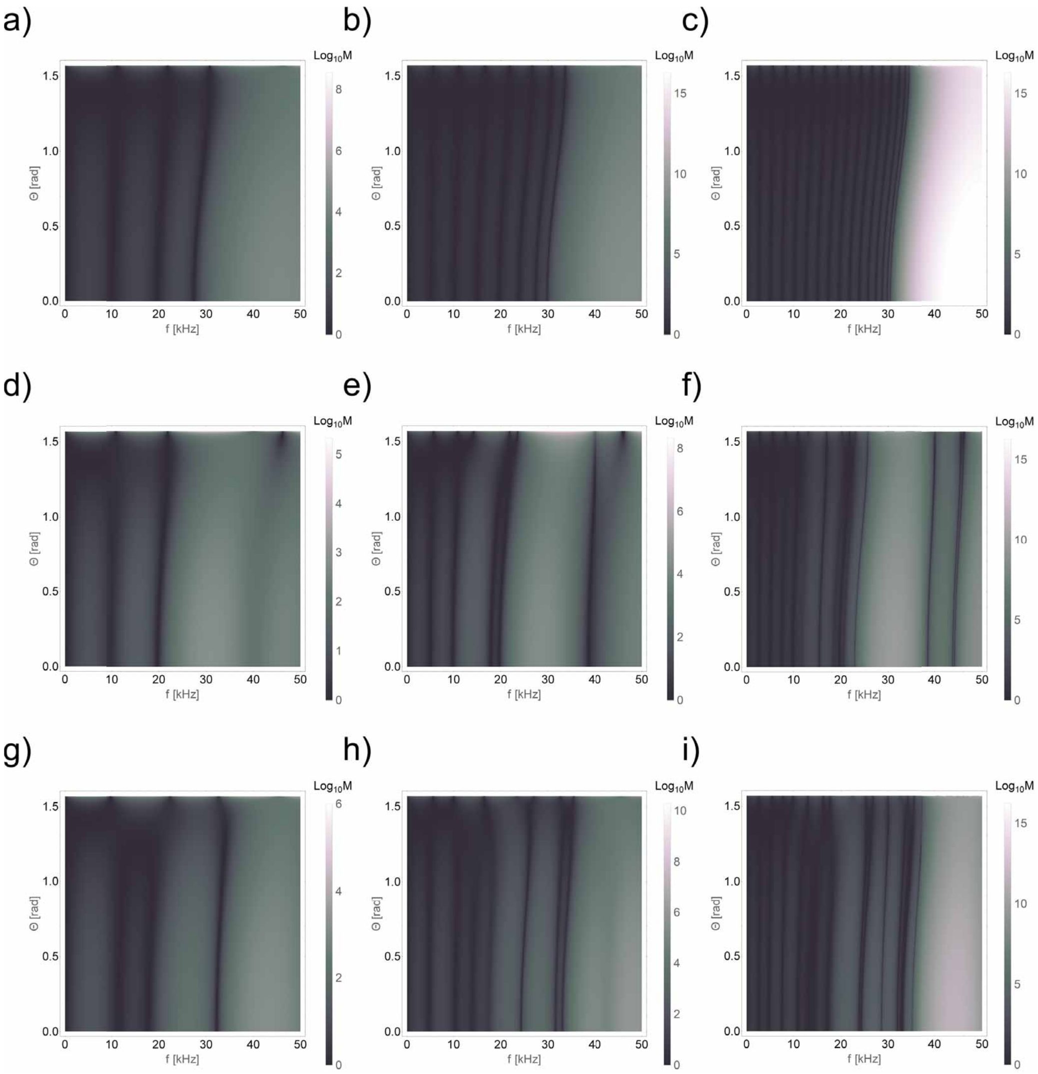

Fig. 7. The $Log_{10}M$ values when material A was epoxy resin and material B an amorphous alloy $Zr_{55}Cu_{30}Ni_5Al_{10}$ depending on the angle of incidence of the wave and frequency for structures: (**a**) X_3^B; (**b**) X_4^B; (**c**) X_5^B; (**d**) X_3^{T-M}; (**e**) X_4^{T-M}; (**f**) X_5^{T-M}; (**g**) X_3^S; (**h**) X_4^S; (**i**) X_5^S

the reflectance for L equal to 4, but no changes were observed for generation numbers 3 and 5. The nature of the reflectance distribution of the analyzed multilayers is complex, so it is reasonable to use for designing structures with given properties the optimization algorithms (e.g. genetic algorithm).

REFERENCES

[1] M.N. Armenise, C.E. Campanella, C. Ciminelli, F. Dell'Olio, V.M.N. Passaro, Physcs. Proc. **1** (3), 357-364 (2010), DOI: 10.1016/j.phpro.2010.01.047

[2] M. Sigalas, E.N. Economou, J. Sound Vib. **158** (2), 377-382 (1992), https://doi.org/10.1016/0022-460X(92)90059-7

[3] S. Kushwaha, P. Halevi, L. Dobrzynski, B. Djafari-Rouhani, Phys. Rev. Lett. **71** (13), 2022-2025 (1993), https://doi.org/10.1103/PhysRevLett.71.2022

[4] M.S. Kushwaha, Int. J. Mod. Phys. B **10**, 977-1094 (1996).

[5] Y. Tanaka, T. Yano, S.-I. Tamur, Wave Motion **44**, 501-512 (2007), https://doi.org/10.1016/j.wavemoti.2007.02.009

[6] Y. Pennec, B. Djafari-Rouhani, H. Larabi, J. Vasseur, A.-C. Hladky-Hennion, Phys. Status Solidi C **6** (9), 2080-2085 (2009), DOI: 10.1002/pssc.200881760

[7] Y.F. Li, F. Meng, S. Li, B. Jia, S. Zhou, X. Huang, Phys. Lett. A **382** (10), 679-684 (2018), https://doi.org/10.1016/j.physleta.2017.12.050

[8] V. Pennec, J.O. Vasseur, B. Djafari-Rouhani, L. Dobrzyński, P.A. Deymier, Surf. Sci. Rep. **65** (8), 229-291 (2010), DOI: 10.1016/j.surfrep.2010.08.002

[9] X.F. Li, X. Ni, L.A. Feng, M.H. Lu, C. He, Y.F. Chen, Phys. Rev. Lett. **106**, 084301 (2011), https://doi.org/10.1103/PhysRevLett.106.084301

[10] A. Khelif, A. Choujaa, S. Benchabane, B. Djafari-Rouhani, V. Laude, Appl. Phys. Lett. **84**, 4400 (2004), https://doi.org/10.1063/1.1757642

[11] D. Richards, D. Pines, J. Sound Vib. **264**, 317-342 (2003), DOI: 10.1016/S0022-460X(02)01213-0

[12] M. Kafesaki, M.M. Sigalas, N. García, Phys. Rev. Lett. **85** (19), 4044-4047 (2000), https://doi.org/10.1103/PhysRevLett.85.4044

[13] J.V. Sanchez-Perez, C. Rubio, R. Martinez-Sala, R. Sanchez-Grandia, V. Gomez, Appl. Phys. Lett. **81** (27), 5240-5242 (2002), DOI: 10.1063/1.1533112

[14] S. Alagoz, O.A. Kaya, B.B. Alagoz, Appl. Acoust. **70**, 1400-1405 (2009), doi:10.1016/j.apacoust.2009.06.001

[15] O.R. Bilal, M.I. Hussein, Phys. Rev. E **84** (6), 065701 (2011), DOI: 10.1103/PhysRevE.84.065701

[16] L. Sanchis, F. Cervera, J. Sánchez-Dehesa, J.V. Sánchez-Pérez, C. Rubio, R. Mártinez-Sala, J. Acoust. Soc. Am. **109**, 2598-2605 (2001),DOI: 10.1121/1.1369784

[17] S. Garus, W. Sochacki, J. App. Math. Comp. Mech. **17** (4), 19-24 (2018), DOI: 10.17512/jamcm.2018.4.03

[18] V.M. García-Chocano, S. Cabrera, J. Sánchez-Dehesa, Appl. Phys. Lett. **101**, 184101 (2012), https://doi.org/10.1063/1.4764560

[19] S.M. Dimitrijevi´c, V.M. García-Chocano, F. Cervera, E. Roth, J. Sánchez-Dehesa, Materials **12**, 2806 (2019), DOI: 10.3390/ma12172806

[20] F. Morandi, M. Miniaci, A. Marzani, L. Barbaresi, M. Garai, Appl. Acoust. **114**, 294-306 (2016), DOI: 10.1016/j.apacoust.2016.07.028

[21] X. Yu, Z. Lu, T. Liu, L. Cheng, J. Zhu, F. Cui, J. Sound Vib. **449**, 140-156 (2019), https://doi.org/10.1016/j.jsv.2019.02.042

[22] W.-Q. Zhang, X. Zhang, F.-G. Wu, Y.-W. Yao, S.-F. Lu, H.-F. Dong, Z.-F. Mu, J.-B. Li, Phys. Lett. A **382**, 423-427 (2018), DOI: 10.1016/j.physleta.2017.12.014

[23] O. Dazel, J.P. Groby, B. Brouard, C. Potel, J. Appl. Phys. **113**, 083506 (2013), http://dx.doi.org/10.1063/1.4790629

[24] S. Garus, W. Sochacki, M. Bold, Engineer. Mechan. 229-232 (2018), doi: 10.21495/91-8-229

[25] M.M. Sigalas, C.M. Soukoulis, Phys. Rev. B **51**, 2780 (1995), https://doi.org/10.1103/PhysRevB.51.2780

[26] P.G. Luan, Z. Ye, Phys. Rev. E **63** (6), 066611 (2001), https://doi.org/10.1103/PhysRevE.63.066611

[27] S. Garus, W. Sochacki, J. App. Math. Comp. Mech. **16** (4), 17-27 (2017), DOI: 10.17512/jamcm.2017.4.02

[28] M.I. Pop, N. Cretu, Wave Motion **65**, 105-111 (2016), https://doi.org/10.1016/j.wavemoti.2016.04.011

[29] J. Madrigal-Melchor, A. Enciso-Muñoz, D. Contreras-Solorio, X. Saldaña-Saldaña, R.A. Reyes-Villagrana, Open Journal of Acoustics **7**, 39-51 (2017) doi: 10.4236/oja.2017.73005

[30] K. Gruszka, M. Nabiałek, M. Szota, K. Bloch, J. Gondro, P. Pietrusiewicz, A.V. Sandu, A.M. Mustafa Al. Bakri, S. Walters, K. Walters, S. Garus, M. Dośpiał, J. Mizera, Arch. Metall. Mater. **61** (2), 641-644 (2016), DOI: 10.1515/amm-2016-0109

[31] K. Bloch, M. Nabiałek, M. Dośpiał, S. Garus, Arch. Metall. Mater. **60** (1), 7-10 (2015), DOI: 10.1515/amm-2015-0001

[32] S. Garus, M. Nabiałek, J. Garus, Acta Phys. Pol. A **126** (4), 960-962 (2014). DOI: 10.12693/APhysPolA.126.960

[33] F. Mikio, W. Xinmin, I. Akihisa, J. Non Cryst. Solids **356** (33-34), 1707-1710 (2010), https://doi.org/10.1016/j.jnoncrysol.2010.06.025

[34] Y. Wang, W. Song, E. Sun, R. Zhang, W. Cao, Physica E Low Dimens. Syst. Nanostruct. **60**, 37-41 (2014) https://doi.org/10.1016/j.physe.2014.02.001

[35] M. Severin, M. Dulea, R. Riklund, J. Phys.: Condens. Matter. **1**, 8851-8858 (1989), https://doi.org/10.1088/0953-8984/1/45/010

[36] D. Huang, G. Gumbs, M. Kolář, Phys. Rev. B **46** (18), 11479-11486 (1992), doi:10.1103/physrevb.46.11479

[37] M. Wolkesson, Evaluation of impedance tube methods – A two microphone in-situ method for road surfaces and the three microphone transfer function method for porous materials, Chalmers University of Technology, Göteborg, Sweden 2013.